FATIGUE LIFE PREDICTION USING VISCO-ELASTIC ANALYSIS

Geoffrey M. Rowe and Stephen F. Brown
SWK Pavement Engineering, Inc.
75 Claremont Road
Bernardsville, NJ 07924

Abstract. Several pavements were tested with a wheel tracking device to determine the fatigue performance. The use of the visco-elastic method (with a dissipated energy criteria) was compared to elastic analysis for those pavements tested. Strains measured in test tracks show that, in the longitudinal direction, compressive strains occur which are followed by a tensile peak and then compressive strains again, whereas, in the transverse direction, the strain is all tensile. If a visco-elastic model is employed, non-symmetrical stress/strain responses can be calculated. Further analysis illustrates that using asphalt material properties associated with a visco-elastic model the effect of multiple wheel passes on the strain response could be explained with reasonable accuracy. Analysis of pavements produced a similar ranking to the performance obtained in the test pavements and indicated that as temperature is increased, life decreases, consistent with fatigue calculations by other techniques.

Keywords. Visco-elastic analysis, fatigue, dissipated energy.

INTRODUCTION

Asphalt pavements have traditionally been analyzed using elastic theory to compute the tensile strain at the underside of the bound layer in order to assess the number of load applications likely to initiate fatigue cracking (Shell Int. Pet. Co., 1978, Asphalt Institute, 1982, Brown et al., 1985). An alternative approach described by Rowe et al. (1995) is to use the dissipated energy method but this requires that the pavement be analyzed using visco-elastic theory.

As part of the work presented in this paper several large asphalt slabs were tested under repeated moving wheel loads in a regime simulative of the field situation. The experimental arrangement, previously described by Rowe and Brown (1997) is shown in Figure 1.

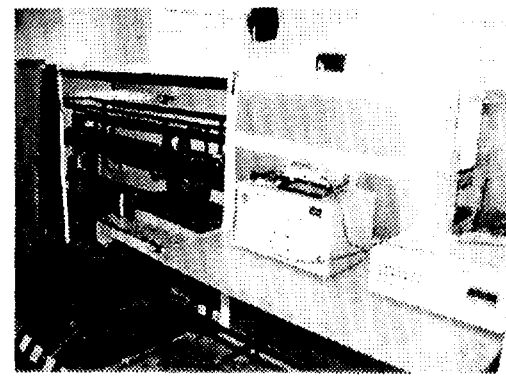

Figure 1 : General Experimental Arrangement for the Fatigue Wheel Tracking Apparatus

Their fatigue performance was then compared with predictions using both analysis methods. In addition, strain measurements from full-scale trails were used to assess the validity of the visco-elastic theory, developed by Rowe et al. (1995). Their computer program allows a number of parallel Maxwell elements to be used in modelling the asphalt layer as shown in Figure 2.

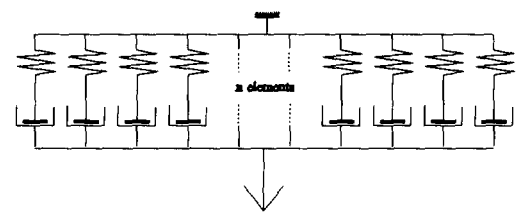

Figure 2 : Generalized Maxwell Model

THE CASE FOR VISCO-ELASTIC ANALYSIS

Huhtala et al. (1990) reported strains measured in a test track. These showed that, in the longitudinal direction, compressive strains occur which are followed by a tensile peak and then compressive strains again, whereas, in the transverse direction, the strain is all tensile (see Figures 2 and 3). In the transverse direction, there is a residual strain following the passage of the wheel load, whereas in the longitudinal direction there are differences in the magnitude of the compressive strain that occurs before and after the tensile peak. If linear elastic analysis is used, the shape of the resulting strain curves are symmetrical. Therefore, Huhtala et al. (1990) presented strong evidence to suggest that linear elastic analysis is not appropriate for computing the strains (and indirectly, stresses) in an asphalt pavement structure under the passage of a wheel load. However, if a visco-elastic model is employed, non-symmetrical stress/strain responses can be calculated as illustrated in Figures 5 and 6. In this example, the material model for the asphalt layers uses two Maxwell elements in parallel and resulted from use of the finite element program.

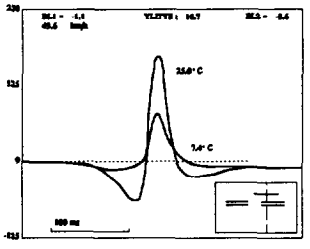

Figure 3 : Longitudinal Strains at underside of bound layer (after Huhtala et al., 1990)

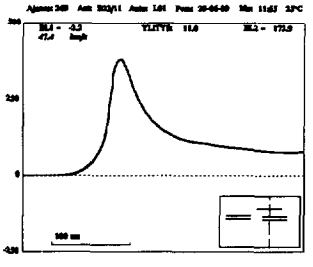

Figure 4 : Transverse Strains at underside of bound layer (after Huhtala et al., 1990)

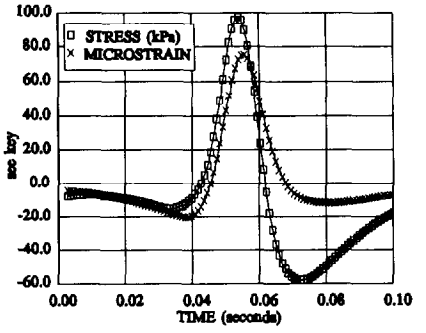

Figure 5: Longitudinal Stresses and Strains

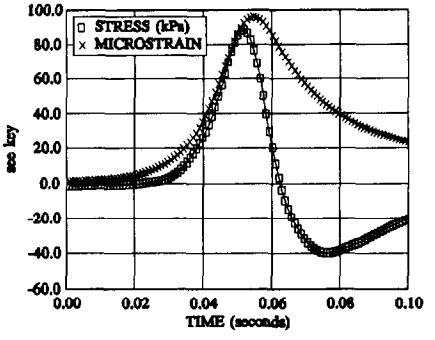

Figure 6: Transverse Stresses and Strains

The curves in these figures have the same basic shape as observed by Huhtala et al. (1990). A further analysis by Huhtala et al. (1992) illustrated that using asphalt material properties associated with the Burgers' model the effect of multiple wheel passes on the strain response could be explained with reasonable accuracy. The Burgers' model parameters used by Huhtala et al. (1992) were estimated from a procedure developed by Gerritsen (1987) which makes use of the binder stiffness and other mixture properties as given by the following Equations:

$$\log E_1 = 1.185 + 0.479 \log S_{bit} - 0.072\ VMA \qquad (1)$$

$$\log E_2 = 0.203 + 1.021 \log S_{bit} - 0.083\ VMA \qquad (2)$$

$$\log V_1 = 2.174 - 1.634 \log Pen \quad (3)$$

$$\log V_2 = 0.796 \log E2_{pred} - 1.083 \quad (4)$$

where: E_1, E_2, V_1 and V_2 are the Burger parameters (E = spring stiffness, V = dashpot viscosity) (E_1, V_1 a Maxwell element and E_2, V_2 a Kelvin element)

It should be noted that there is a direct equivalency between the Burgers' model and two Maxwell elements acting in parallel, as follows:

$$E_1 = E_I + E_{II} \quad (5)$$

$$E_2 = \frac{A\,(E_I + E_{II})}{B\,(E_I + E_{II}) - A} \quad (6)$$

$$V_1 = V_I V_{II}\left(\frac{1}{V_I} + \frac{1}{V_{II}}\right) \quad (7)$$

$$V_2 = \frac{(E_I + E_{II})^2}{(E_I + E_{II})\,B - A} \quad (8)$$

where:

$$A = E_I E_{II}\left(\frac{1}{V_I} + \frac{1}{V_{II}}\right) \quad (9)$$

$$B = \left[\left(\frac{E_I}{V_I} + \frac{E_{II}}{V_{II}}\right) - \frac{(E_I + E_{II})\left(\frac{E_I E_{II}}{V_I V_{II}}\right)}{A}\right] \quad (10)$$

and

E_I, E_{II}, V_I and V_{II} are the parameters associated with two Maxwell elements in parallel

If stress and strain are both calculated then they can be plotted to obtain hysteresis loops as shown in Figures 7 and 8. In addition, the Finite Element code enables direct computation of deviatoric dissipated energy and a typical contour plot of this parameter following the passage of a single wheel load is shown in Figure 9. The contour plot shows that peak dissipated energy occurs under the wheel load with high values also in areas near the edge of the load. Full details of this pavement are given in Table 1. In this situation fatigue cracking will be initiated at the underside of the pavement. The peak value of dissipated energy at this location is 38.5 Joules/m^3.

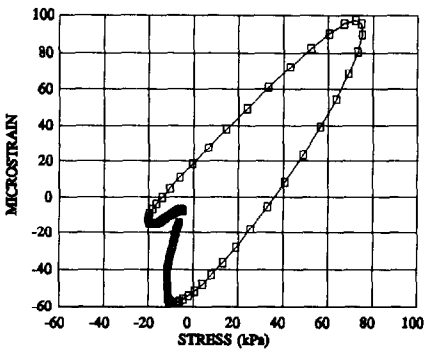

Figure 7: Calculated Longitudinal Hysteresis Loop at underside of bound layer

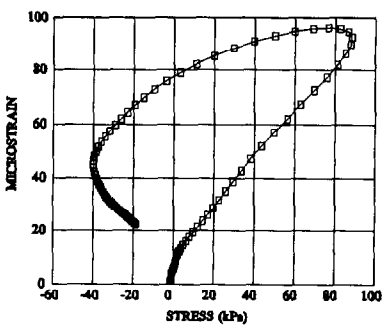

Figure 8: Calculated Transverse Hysteresis Loop at underside of bound layer

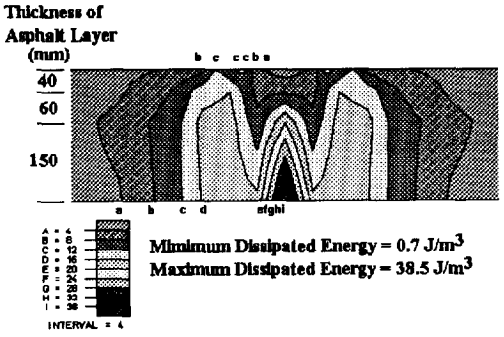

Figure 9: Fatigue Damage Contour

Table 1 : Details of Typical 250 mm Thick Pavement

Material Layers and Properties		
Layer	Thickness (mm)	Properties
Hot Rolled Asphalt Wearing Course	40	E_i = 406.7 MPa V_i = 747.9 MPa.sec E_{ii} = 1273.3 MPa V_{ii} = 32.1 MPa.sec
Hot Rolled Asphalt Basecourse	60	E_i = 355.0 MPa V_i = 539.7 MPa.sec E_{ii} = 1,835.0 MPa V_{ii} = 33.0 MPa.sec
Dense Bitumen Macadam Base	150	E_i = 508.4 MPa V_i = 741.2 MPa.sec E_{ii} = 2,541.6 MPa V_{ii} = 33.0 MPa.sec
Pavement Foundation	3,570	E = 200 MPa
Wheel load = 20 kN Contact Pressure = 600 kPa Load Pulse Duration = 9.27 ms Visco-elastic properties for the asphaltic materials were calculated using the procedures developed by Gerritsen (1987).		

FINITE ELEMENT MODEL

The computer program, PACE, developed by Rowe et al. (1995) for fatigue life prediction consists of a "core"

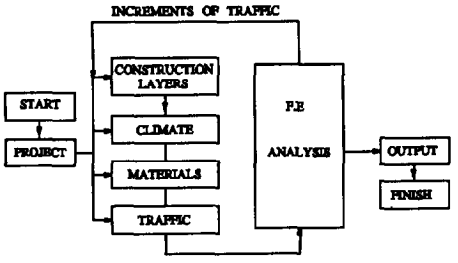

Figure 10 : Finite Element Program Elements

FE program which interacts with other programs and subroutines that provide information on material properties, pavement temperatures and traffic conditions as illustrated in Figure 10. The greater part of the existing finite element code, initially drawn upon for program development, is based on work described by Owen and Hinton (1980) and was coded by Sharrock (1990). The principle assumptions made in the FE code are described below.

Visco-elastic materials are treated as a special case of visco-elastic-plastic behavior, in which the yield stress in the plastic slider element, for the onset of visco-plasticity, is reduced to zero (see Figure 11). Elastic material behavior is also obtained as a special case, by specifying a very large yield stress for the plastic element so that visco-plastic flow cannot occur. Linear isotropic elasticity is assumed for modelling elastic behavior with Young's modulus and Poisson's ratio used to characterize the material.

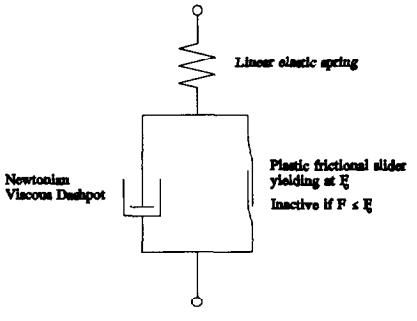

Figure 11 : Rheological Representation of Model Employed

The total strain is assumed to be separable into elastic and visco-plastic components and, in terms of strain rates, as follows:

$$\dot{\epsilon} = \dot{\epsilon}_e + \dot{\epsilon}_{vp} \quad (11)$$

where: $\dot{\epsilon}$ = total strain rate

$\dot{\epsilon}_e$ = strain rate associated with elastic behavior

$\dot{\epsilon}_{vp}$ =strain rate associated with visco-plastic behavior

The elastic component is assumed to experience the total stress acting and, therefore, the total stress rate depends on the elastic strain rate by way of the elasticity matrix D:

$$\dot{\sigma} = D\,\dot{\epsilon}_e \quad (12)$$

The visco-plastic strain rate is determined from the current state of stress by the relationship:

$$\dot{\epsilon}_{vp} = \gamma \cdot [\mathcal{F}(F)] \cdot \frac{\partial F}{\partial \sigma} \quad (13)$$

In Equation 13 $\partial F/\partial\sigma$ represents a plastic potential and γ is a fluidity (reciprocal of viscosity). The yield function F is that of Von Mises and the function $\mathcal{F}(F)$ is given by:

$$\mathcal{F}(F) = \frac{F - \sigma_y}{\sigma_y} \quad (14)$$

For the case of purely viscous flow, with zero yield stress for plasticity:

$$\mathcal{F}(F) = F \quad (15)$$

The resulting viscous strain increment is assumed to be entirely deviatoric (ie. shear with no volume change) and proportional to the current deviator stresses. The mixture "viscosity" is a shear viscosity in these circumstances. This is considered to lead to a reasonable approximation of viscous flow with viscous or visco-elastic material behavior.

Asphaltic materials cannot be characterized by the basic visco-elastic-plastic model used in the FE program as shown in Figure 11 but require more complex models to explain their behavior. A method of obtaining more realistic material response, in the context of FE modelling, is to build up a composite action by using a number of different 'overlays' of simpler materials each with different characteristics. The material to be analyzed is assumed to be composed of several layers each of which undergoes the same deformation (strain compatibility). The total stress field in the material is then obtained by a summation to which each part of the 'overlay' contributes in proportion to the fractional weighting allocated in the total material. In a two dimensional situation, the total thickness is taken to be unity and the weighting for each material simply equals its thickness in the overlay (Zienkiewicz et al, 1972; Owen et al., 1974, and Pande et al., 1977). This concept is illustrated in Figure 12. The current version of the software (PACE Version 1.11, 7/3/95) uses a plain strain analysis. In order to produce deflections of the same magnitude as a full 3D analysis, the stiffness of the elastic base layers (sub-base and sub-grade) are increased by a factor of five. This factor was determined by conducting both 2D and 3D Finite Element analysis and was applied to the sub-base and subgrade in the 2D calculations which resulted in the same values of dissipated energy in the asphaltic materials that were obtained in the 3D case. This adjustment produces similar values of dissipated energy when using the plain strain analysis compared to a 3D analysis.

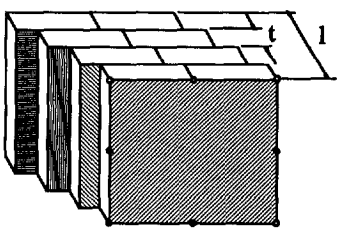

Unit thickness overlay composed of 4 materials, 2-D situation

Figure 12 : 'Overlay' Model

VISCO-ELASTIC MATERIAL PROPERTIES

Relaxation properties. A method of analysis has been implemented to obtain a model which will allow input of parameters associated with a generalized Maxwell model, Figure 2. The current version uses properties associated with a four element Maxwell model for the fatigue life calculations. With 4-10 elements, excellent fits were obtained for the prediction of frequency sweep data over a wide range of loading times (Bouldin et al., 1994). The material properties are obtained from a computer program developed by Sharrock (1994) which determines a discrete relaxation spectrum for input

consisting of frequency sweep data. The data is reduced to four sets of Maxwell parameters which can describe the complex properties of the material. A comparison between using two Maxwell units and four Maxwell units to describe a frequency sweep data set is illustrated in Figures 13 and 14. It can be seen that if two units are used, then it is only possible to fit the data well at two specified frequencies while, if four are used then a good fit is obtained over two decades of frequency.

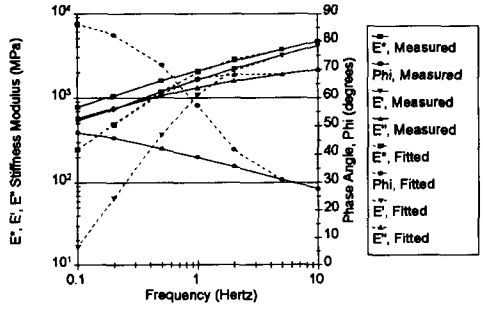

Figure 13: Complex Properties Measured and Fitted with Two Maxwell Elements in Parallel

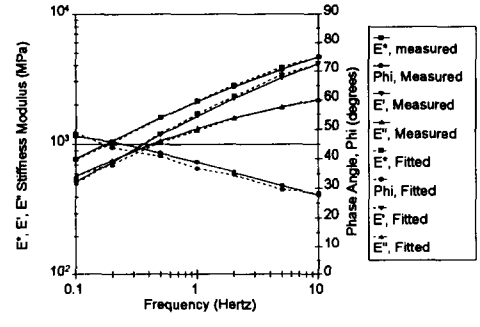

Figure 14: Complex Properties Measured and Fitted with Four Maxwell Elements in Parallel

Shear frequency sweep data. Tayebali et al. (1994) proposed a method of fatigue prediction based upon shear frequency sweep data using the Superpave Shear Tester (SST) and elastic analysis. Since the SST is being introduced into U.S. practice it is considered desirable to investigate the use of this data in a prediction procedure. Relationships were proposed for conversion of the shear data to flexural data as follows:

$$S_o = 8.560\ (G_o)^{0.913} \qquad (r^2 = 0.712) \quad (16)$$

$$S_o'' = 81.125\ (G_o'')^{0.725} \qquad (r^2 = 0.512) \quad (17)$$

$$\sin \delta_{S_o} = 1.040\ (\sin \delta_{G_o})^{0.725} \qquad (r^2 = 0.810) \quad (18)$$

where S_o = Stiffness modulus, bending beam test.
S_o'' = Loss Stiffness modulus, bending beam test.
G_o = Stiffness modulus, shear test.
G_o'' = Loss Stiffness modulus, shear test.
δ = Phase lag (subscript indicates type of test).

The shear data were measured using the SHRP Test Method M-003 (Harrigan et al., 1994). This test method requires that the specimen height remains constant. This results in the application of an axial load in addition to the applied shear load. The test is conducted at a constant shear strain amplitude of 100 με.

In the comparison of shear and flexural data, it can be assumed that the relationship for the phase angle should pass through the ordinates (0,0) and (90,90) representing purely elastic and viscous behavior respectively. However, the relationship proposed above (Tayebali et al., 1994) is a power law which will result, for higher phase angles, in a mathematical error (sin δ > 1) if it is used for conversions. Since, a generalized relationship was needed for the visco-elastic model, a study was performed to fit a physical relationship which can be used over the entire range of possible phase angles thus permitting extrapolation from the original data set. It was considered that the best description of the data (forcing the relationship through the two ordinates discussed above) could be obtained using a sine function. An iterative analysis was performed (minimizing the root mean square error) giving the following result:

$$\delta_{S_o} = \delta_{G_o} + 9.65\ (\sin 2\delta_{G_o}) \qquad (19)$$

This result, which has a rms error value of 1.78 degrees compared to 1.88 degrees for the SHRP equation and 1.85 degrees for a linear best fit, is illustrated in Figure 15 along with the other relationships.

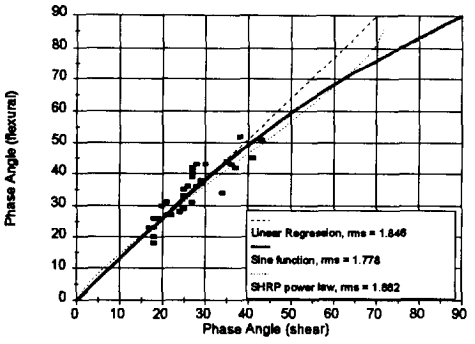

Figure 15: Phase Angle Measurements, Flexural vs. Shear

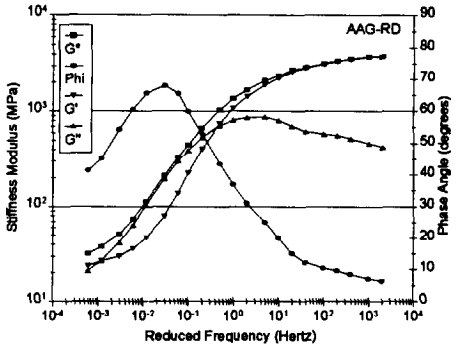

Figure 17: Master Curve Reduced to 20°C for Mixture AAG-RD in Simple Shear

The flexural and shear stiffnesses are related by a factor of three as illustrated in Figure 16. Shear frequency sweep data were published Tayebali et al. (1994) for each of the six slabs tested in the University of Nottingham Slab Test Facility (Rowe and Brown). These results have been analyzed to determine the Maxwell parameters at 20°C. In addition, it is also possible to construct master curves, shift these to any desired temperature and then predict a discrete relaxation spectrum (for four Maxwell elements) at that temperature. Figure 17 illustrates the master curve obtained for mixture AAG-RD. This has been shifted to temperatures between 4°C and 40°C and the discrete relaxation spectrum calculated at each temperature. The results for this analysis are illustrated in Figures 18 and 19.

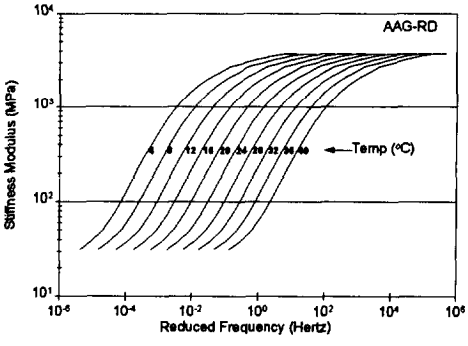

Figure 18: Complex Stiffness Modulus for Mix AGG-RD between 4°C and 40°C

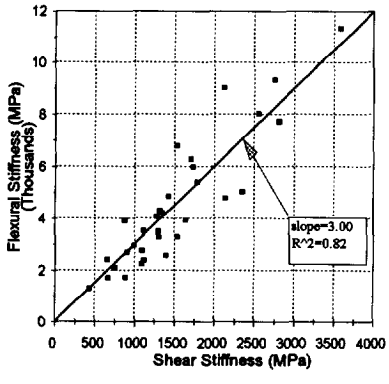

Figure 16 : Relationship Between Shear and Flexural Stiffness

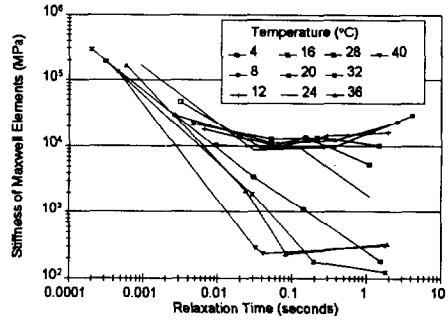

Figure 19: Discrete Relaxation Spectrum for Various Temperatures for Mix AAG-RD

ANALYSIS OF THE SLAB TEST EXPERIMENT

Visco-elastic analysis. The Slab test experiments conducted in the apparatus shown in Figure 1 were analyzed by the PACE™ visco-elastic FE analysis software at the load levels used in the experiment. For each slab, a dissipated energy contour map was generated. The significant variables used for this analysis were as follows:

Base Support:	10 MPa stiffness rubber mat 92 mm thickness resting on a steel base with assigned stiffness of 500,000 MPa (ie. very stiff) 4.0 m thickness.
Temperature:	Constant with depth, 20°C.
Wheel speed:	2.3 km/hr.
Wheel load:	Range 0.8 to 4.5 kN.
Contact pressure:	380 kPa.

The asphaltic material properties were based upon shear frequency sweep results as discussed earlier. An example of the dissipated energy contour plot (mixture AAF-RD) produced by the software is presented in Figure 20. By inspection it can be seen that the maximum value of dissipated energy occurs at the underside of the asphaltic layer and this was true for all mixtures analyzed in these experiment. This value of dissipated energy was then used to estimate the fatigue life to crack initiation, *N1*, as follows:

$$N1 = 205 \times Vb^{6.44} \times w_o^{-2.01} \times \Psi_{N1}^{1.64} \qquad (20)$$

[Vb (%) and w_o (J/m^3)]

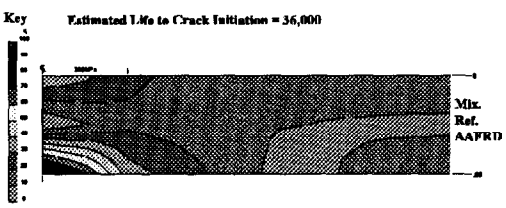

Figure 20: Fatigue Damage Factor

The FE analysis, generally, ranked the materials in the same order as the results obtained from the experiments with the exception of mixture AAK-RD (see Figure 21). The difference between the calculated lives versus that measured in the STF (both at the *N1* stage) are considered to be a result of rest periods which occurred in the experiment. The fatigue relationship used in the calculations (see Equation 20) was based on fatigue testing which contained no rest periods. Figure 22, which presents the data graphically, includes a line which represents a shift factor of ×25 as suggested by Raithby (1972) to account for rest periods. This line lies in the center of the data collected. A regression line (excluding AAK-RD) is also shown and this indicates that the difference, in the measured and predicted results, is greater for slabs with longer lives. An alternate interpretation is that different shift factors apply for short and long fatigue lives. Shift factors based upon this data are illustrated in Figure 23. The mean shift factor for the long fatigue life results (AAA, AAF, AAK and AAM-RD) was 64 whereas that obtained for the shorter lives (AAC and AAF-RD) was 6.

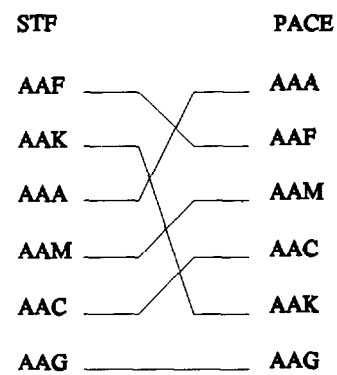

Figure 21: Rankings in the Slab Experiment and by using Visco-Elastic Analysis

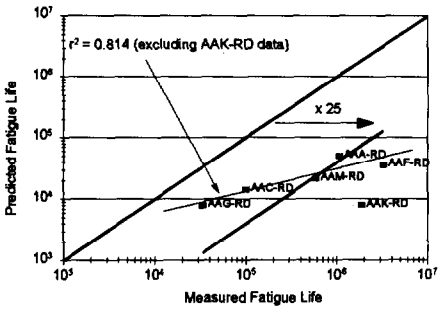

Figure 22: Calculated vs. Observed Results for the Slab Experiments

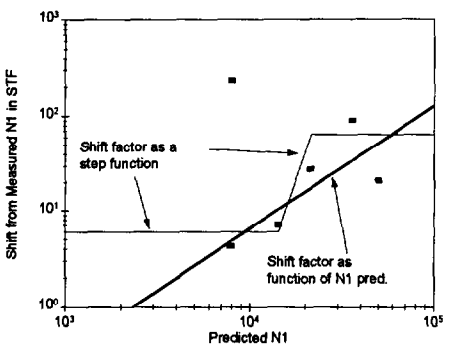

Figure 23: Shift factor as a Step Function or as a Function of Predicted *N1*

Comparison with elastic analysis: Using the load and mixture stiffness appropriate for the slab experiments, the fatigue life was calculated using strain — life relationships and layered elastic analysis. The strain life relationships were obtained from analysis of controlled stain fatigue test data obtained by the University of California (Tayebali, 1991) on the same mixture. The stiffness values used, along with the constants for the fatigue equation, are given in Table 2 along with the constants used in Equation 21.

$$N_{fat} = k1\ (\epsilon_t)^{k2} \qquad (21)$$

Table 2 : Mixture Properties used for Elastic Analysis

Mixture Reference	Stiffness, E* (MPa)	k1	k2
AAA-RD	2978.1	3.61e-06	-3.1595
AAC-RD	3700.9	2.18e-07	-3.38268
AAF-RD	7363.2	1.58e-07	-3.3854
AAG-RD	5967.2	3.06e-09	-3.77549
AAK-RD	2977.8	3.33e-10	-4.30375
AAM-RD	5868.6	3.36e-09	-4.04387

The results from the viscoelastic analysis are illustrated in Figure 24 and are compared to the elastic analysis in Figure 5. It can be observed that whereas the visco-elastic procedure under-predicted the fatigue life by a factor of twenty five the elastic analysis over-predicts by a similar amount. Clearly, some of the differences could be attributed to the use of controlled strain fatigue data for the conditions in the experiment which were closer to the controlled stress mode of loading. Both visco-elastic and elastic analysis appear to rank the data in a similar manner but this result indicates that considerable care needs to be given to the choice of controlled stress versus controlled strain fatigue data. The energy method can, potentially, overcome this problem and use of the test type would not effect the position of the estimated life to crack initiation.

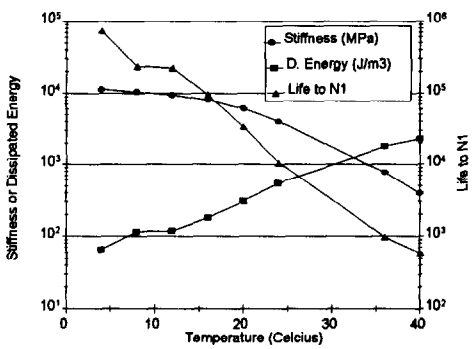

Figure 24: Results from Visco-elastic Analysis of the SLab Mix AAG-RD

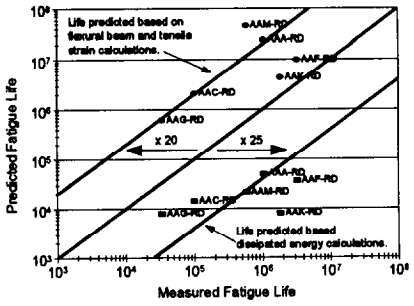

Figure 25: Fatigue Life Predictions

Pavement thickness and temperature. To investigate the effect of stiffness and temperature with the dissipated energy method, a series of calculations where performed for; 1) the slab experiments, 2) a typical thick pavement structure, and 3) a typical thin pavement structure. All the calculations used mixture AAG-RD at different temperatures. The visco-elastic material properties were those presented in Figure 18. In addition, computations were made using the University of Nottingham design method (Brown et al., 1985) but with the mixture stiffness values calculated using the Bonnaure nomograph (Bonnaure et al., 1977). The life calculations use the fatigue relationship developed by Cooper (1976) without any shift factors to allow for differences between element test slab loading case. The parameters used for the calculations are presented in Table 3.

Anticipated effect of temperature on the experimental results. The results obtained for the simulation of the slab experiments at varying temperatures are presented in Figure 24. It can be clearly observed that, in this experiment, as the stiffness of the asphaltic material drops, the amount of dissipated energy increases and the calculated fatigue life decreases.

Effect of temperature on typical thick and thin pavements. The results from the visco-elastic analysis and elastic analysis of the "thick" and "thin" pavements with "weak" and "strong" foundations" are presented in Figure 26. It can be observed that in all cases the fatigue life to crack initiation (N1) generally decreases with increasing temperature. The result suggests that a stiffer material performs better in the prevention of

Table 3 : Parameters used in Elastic and Visco-Elastic Comparison Study

Mixture Properties (AAG-RD)	
Volumetrics	
Voids Content (%)	9.9
Volume of Binder (%)	11.7
Voids in Mineral Aggregate(%)	21.5
Temperature (°C)	Stiffness(MPa)
4	16799
8	14004
12	10407
16	7352
20	4935
24	3009
28	1825
32	1050
Structure Features	
Layer Thickness (mm)	
Thin Pavement	50
Thick Pavement	300
Foundation Stiffness (MPa)	50 and 300
Loading	
Wheel Arrangement	Dual
Speed of Loading (km/hr)	50
Radius of Loaded Area (mm)	113
Spacing of wheel centers (mm)	376

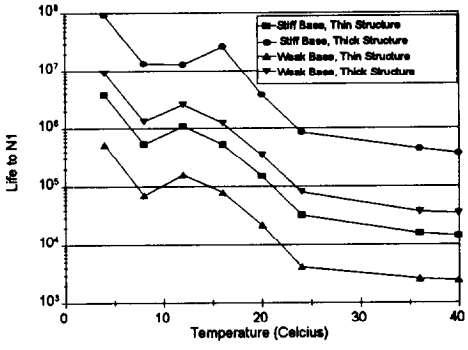

Figure 26: Predicted Life using Visco-Elastic Analysis for Thick and Thin Pavement Structures on Weak and Strong Bases

crack initiation for both thin and thick pavement structures. Figure 27 illustrates a comparison between the life calculated by the two analysis methods including the slab experiments using both PACE™ and UCB data. It can be observed that the lives calculated for the thick pavement are relatively close (within ½ decade for lives 10,000 to 10,000,000). However, the life calculated for the thin pavement structures by elastic analysis is considerably lower than the life calculated by visco-elastic analysis.

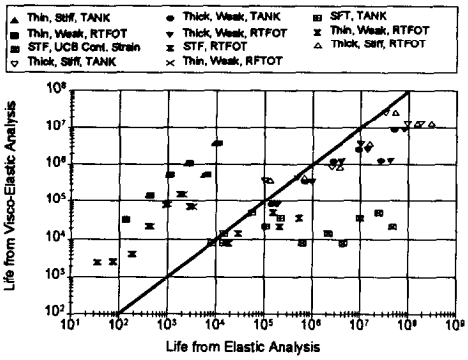

Figure 27: Comparison of Various Structures, Elastic versus Visco_Elastic Analysis, Mix AAG-RD

Thick and thin pavements versus the Experimental results. The results presented in Figure 27 show that the fatigue lives calculated for the thick pavement section have a similar trend line to that obtained for the experimental analysis. This demonstrates that the visco-elastic analysis and elastic analysis using the Nottingham fatigue relationship (Cooper, 1976) give results which are similar (differing by about a ½ decade) for relatively thick pavement structures. For thinner pavement structures the tensile strain relationship results in low calculated lives compared to the visco-elastic analysis.

OTHER COMPARISONS TO ELASTIC ANALYSIS

In order to present further comparison between the viscoelastic theory/dissipated energy approach and elastic theory/tensile strain method use was made of the simplified elastic design method presented by Brown and Brenton (1985). Calculations were performed using the pavement details given in the five cases contained in examples 1 and 2. The input data for the analysis is summarized in Table 4. All results are compared at the crack initiation stage (i.e. no factors for rest periods, crack propagation or lateral wander were used) for three pavement thicknesses (100, 200 and 300 mm).

Table 4 : Design Parameters used in Comparison to University of Nottingham Method

Mixture properties for asphaltic materials					
Mixture Type	Binder Content (%)	Void Content (%)	VMA (%)	VB (%)	Initial Pen at 25°C
Typical HRA WC	7.9	4	21.8	17.8	50
Typical HRA BC	5.7	5.0	18.1	13.1	50
Typical DBM BC	3.5	10.0	17.9	7.9	100
Modified HRA BC	5.0	4.0	15.7	11.7	50
Modified DBM BC	4.5	6.0	16.4	10.4	50
Poisson's ratio assumed as 0.4 for above mixtures					

Binder properties assumed for typical mixtures				
Initial Properties		Recovered Properties		
Penetration at 25°C	Softening Point (°C)	Penetration at 25°C	Softening Point (°C)	Penetration Index
50	53.6	32.5	58.6	-0.2
100	45.7	65.0	50.6	-0.4

Subbase/Subgrade Properties	
Subbase Thickness (mm)	200
Subbase Stiffness (MPa)	100
Subbase Poisson's Ratio	0.3
Subgrade Stiffness (MPa)	
Example 1	30
Example 2	50
Subgrade Poisson's Ratio	0.4

Design Criteria	
Number of Standard Axles (80 kN, Dual)	
Example 1	40,000,000
Example 2	10,000,000
Tire Pressure (kPa)	500
Wheel center spacing (mm)	376
Radius of loaded area	113
Speed of traffic (km/hr)	60
Design Temp. for Fatigue (°C)	
Example 1	17.3
Example 2	19.6
Wearing Course Present	
Example 1	No
Example 2	Yes

Note: Example 2 considers only the Modified HRA Base

Example 1 results. Example 1 compares four three-layer structures consisting of an asphalt base material, sub-base and subgrade. No wearing course is used in this example. A typical example of a dissipated energy contour plot is given in Figure 28. From this figure, it can be observed that the highest value of dissipated energy occurs at the surface and consequently, if this concept is valid, cracking would be expected to occur at this location first. In the majority of the calculations performed (with the exception of two 300 mm thick pavements) the highest value of dissipated energy was at the surface.

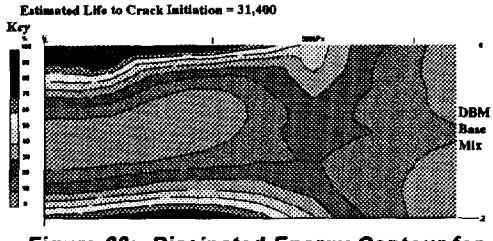

Figure 28: Dissipated Energy Contour for Pavement with Single Layer of DBM, 200 mm Thick

Example 2 results. Example 2 considers a structure which uses a modified HRA base along with a traditional 40 mm HRA wearing course. A typical example of a dissipated energy contour plot for this structure is given in Figure 29. It can be observed that the highest dissipated energy occurs in the less stiff wearing course material. However, unlike the example 1 result, the increased volume of binder in a wearing course results in the crack initiation being expected at the underside of the main structural layer.

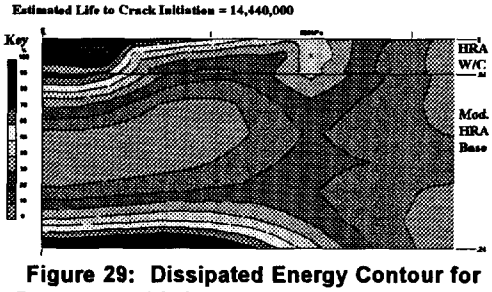

Figure 29: Dissipated Energy Contour for Pavement with 200 mm Thick Modified DBM Base and 40 mm HRA Wearing Course

Visco-elastic properties were estimated using the relationships presented in Equations 1 to 4.

Sensitivity to pavement thickness. The results of the visco-elastic analysis are illustrated in Figure 30. This figure illustrates that the HRA base material has the longest computed life. The results from both analysis techniques are plotted in Figure 31. This illustrates that the life computed from the visco-elastic analysis method is not as sensitive to pavement thickness as the elastic method. However, it also indicates that similar lives are obtained for the thicker pavement structure with the exception of that computed for the DBM base containing the softer 100 pen binder.

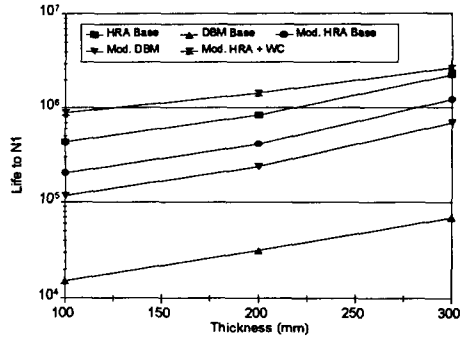

Figure 30: Results Obtained From Visco-Elastic Analysis, Examples 1 and 2

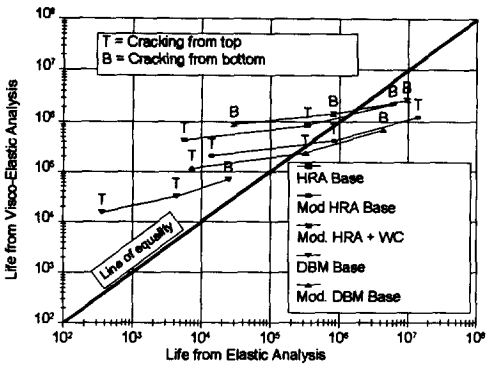

Figure 31: Comparison of Results Between Elastic and Visco-Elastic Analysis

CONCLUSIONS

Various structures have been analyzed using the visco-elastic analysis technique. The analysis required the derivation of visco-elastic material properties from frequency sweep data and from a prediction method. These results were compared to conventional elastic analysis.

The relaxation properties of an asphaltic material can be fitted by a four Maxwell element model to achieve a good fit of properties over a two decade range of frequencies. The fit of a two element model is, in comparison, very poor. An improved method for converting shear frequency sweep data to flexural data was developed. This method enables shear frequency data collected by devices which should be available during the implementation of the SHRP research program to be used. Data from shear testing was used to develop relaxation times for an asphalt mixture in 4°C steps between 4°C and 40°C. In addition, relaxation times at 20°C were obtained for all RD aggregate mixtures.

Visco-elastic analysis of pavements containing aggregate RD produced a similar ranking to the performance obtained in the slab experiments. The results were shifted by a factor of approximately 25 from the actual lives. This difference is considered to be a function of rest periods. The results from controlled strain fatigue testing and elastic analysis over-predicted the fatigue life.

Analysis performed for a pavement with mix AAG-RD at various temperatures indicated that as temperature is increased, life decreases. This result is consistent with fatigue calculations by other techniques.

Analysis of pavements with different section thicknesses suggest that the visco-elastic plain strain analysis is not as sensitive to pavement thickness as the elastic analysis.

DISCLAIMER

This paper represents the views of the authors only and is not necessarily reflective of the views of the National Research Council, the views of SHRP, or SHRP's sponsor. The results reported here are not necessarily in agreement with the results of other SHRP research activities. They are reported to stimulate review and discussion within the research community.

ACKNOWLEDGEMENTS

The authors are very grateful for the support of the University of Nottingham for making available the testing facilities. Professor Peter Pell and Professor Carl Monismith made helpful comments to the original research from which this paper is derived. The help of a large number of technicians and support staff at the University of Nottingham is also acknowledged. Financial support for various elements of the work was provided by SHRP.

REFERENCES

Bouldin, M.G., Rowe, G.M., Sousa, J.B. and Sharrock, M.J., "*Repetitive Creep as a Tool to Determine the Mix Rheology of Hot Mix Asphalt*," Journal of the Association of Asphalt Paving Technologists, Volume 63, 1994, pp. 182 - 223.

Brown, S.F. and Brunton, J.M., "*An Introduction into the Analytical Design of Bituminous Pavements*," 3rd Edition, University of Nottingham, Nottingham, England, 1985.

Brown, S.F., Brunton, J.M. and Stock, A.F., "*The Analytical Design of Bituminous Pavements*," Proceedings, (Paper 8834 Transportation Engineering Group), Institution of Civil Engineers, Part 2, 1985, 79, Mar. 1-31.

Burgers, J.M., "*Mechanical considerations - model systems - phenomenological theories of relaxation and of viscosity*," Academy of Sciences, Amsterdam, first report on viscosity

and plasticity, 1935.

Cooper, K.E., "*The Effect of Mix and Testing Variables on the Fatigue Strength of Bituminous Mixes*," M.Phill Thesis, University of Nottingham, 1976.

Gerritsen, A.H., "*Prediction of The Dynamic Visco-Elastic Behaviour of Asphalt Wearing Course Mixes using Burgers' Model*," Koninklijke/Shell-Laboratorium, Amsterdam, Report MF 88-0809, 1987.

Harrigan, E.T., Leahy, R.B. and Youtcheff, J.S., "*The SUPERPAVE Mix Design System Manual of Specifications, Test Methods, and Practices*," SHRP Report SHRP-A-379, Strategic Highway Research Program, National Research Council, Washington, DC, 1994.

Huhtala, M., Alkio, R., Pihljamaki, J., Pienmaki, M. and Halonan, P., "*Behavior of Bituminous Materials Under Moving Wheel Loads*," Journal of the Association of Asphalt Paving Technologists, Vol. 59, 1990, pp 422-442.

Huhtala, M. and Pihajamäki, J., "*New Concepts on Load Equivalency Measurements*," Proceedings, 7th International Conference on Asphalt Pavements, Volume 3, 1992, pp. 194-208.

Owen, D.R.J. and Hinton, E., "*Finite Elements in Plasticity. Theory and Practice*," Pineridge Press, Swansea, 1980.

Owen, D.R.J., Prakash, A. and Zienkiewicz, O.C., "*Finite Element Analysis of Non-linear Composite Materials by use of Overlay Systems*," Computers and Structures, Vol. 4, 1974, pp. 1251 -1267.

Pande, G.N., Owen, D.R.J., and Zienkiewicz, O.C., "*Overlay Models in Time Dependent Nonlinear Material Analysis*," Computers and Structures, Vol. 7, 1977, pp 435-443.

Raithby, K.D. "*Laboratory Fatigue Tests on Rolled Asphalt and Their Relationships to Traffic Loading, Roads and Road Construction*," August/September 1972, pp. 219-223.

Rowe, G.M., Brown, S.F., Sharrock, M.J. and Bouldin, M.G., "*Visco-Elastic Analysis of Hot Mix Asphalt Pavement Structures*," Paper presented at the Annual Meeting of the Transportation Board, Washington, DC, January, 1995.

Rowe, G.M. and Brown, S.F., "*Validation of the Fatigue Performance of Asphalt Mixtures with Small Scale Wheel Tracking Experiments*," Paper submitted for consideration, AAPT, 1997.

Sharrock, M.J., "*Computer Program to Predict Pavement Performance*," Progress Report Submitted to Shell Development Company, SWK Pavement Engineering, 1990.

Sharrock, M.J., "*Computer Program - Frequency Domain*," PACE™ Software, SWK Pavement Engineering, 1994.

Shell International Petroleum Company "*Shell Pavement Design Manual*," London, 1978.

Tayebali, A., "*Fatigue test results, R^2 for exponential regression fit for dissipated energy versus number of cycles*," A-003A Project Communication between Akhtar Tayebali and Geoff Rowe, November 7, 1991.

Tayebali, A.A., Tsai, B. and Monismith, C.L., "*Stiffness of Asphalt-Aggregate Mixes*," Report SHRP-A-388, Strategic Highway Research Program, National Research Council, Washington, DC, 1994.

The Asphalt Institute, "*Research and Development of the Asphalt Institute Design Manual (MS-1) Ninth Edition*," The Asphalt Institute, RR 82-2, 1982.

Zienkiewicz, O.C., Nayak, G.C. and Owen, D.R.J., "*Composite and Overlay Models in Numerical Analysis of Elasto-plastic Continua*," International Symposium on Foundations of Plasticity, Warsaw, 1972.